Image Noise Reduction Using Structural Mode Shaping for Scanning Electron Microscopy

Mitsuru Hamochi[1,#] and Shinji Wakui[2]

1 JEOL Ltd, 1-2 Musashino 3-Chome Akishima Tokyo 196-8558 Japan
2 Tokyo University of Agriculture and Technology, Tokyo, Japan
Corresponding Author / E-mail: hamochi@jeol.co.jp, Tel: +81-42-542-2264, Fax: +81-42-546-8063

KEYWORDS : Scanning electron microscopy, Mode shape, Natural frequency, Acoustic noise, Resonance

In a scanning electron microscope (SEM), outside acoustic noise causes image noise that distorts observations of the specimen being examined. A SEM that is less sensitive to acoustic noise is highly desirable. This paper investigates the image noise problem by addressing the mode shapes of the base plate and the transmission path of the acoustic noise and vibration. By arranging the position of the rib, a new SEM base plate was developed that had twisting as the 1st and 2nd modes. In those two twisting modes, vibration nodes existed near the center of the base plate where the specimen chamber is placed. Less vibration was transmitted to the chamber and to the specimen by the twisting modes compared to bending ones, which are the 2nd and 3rd modes for a rectangular plain base plate. An SEM with the developed base plate installed exhibited a significant reduction of image noise when exposed to acoustic noises below 250 Hz.

Manuscript received: October 18, 2007 / Accepted: January 7, 2008

1. Introduction

The scanning electron microscope (SEM) is a device for the observation and analysis of the surface of a specimen at a high magnification. It is used in a wide range of applications, from the observation of micro-organisms to inspection processes in semiconductor production. SEMs are often used in offices or clean rooms that have relatively high levels of floor vibration and sound pressure. These cause small vibrations in the SEM. Since the magnification is high, image noise is observable when the relative displacement between the electron beam and the specimen is greater than the resolution of the SEM. Image noise makes it impossible to observe the correct shape of the specimen. The image noise amplitude is influenced by both the frequency profile of the fluctuation and the natural frequencies of the equipment. Those frequencies depend on the geometrical shape and material of the SEM components. Therefore, we investigated the shape of the vibration modes of the SEM structure as well as the associated natural frequencies. This paper focuses on the structure of the SEM base plate. We discovered that image noise in a SEM is caused by the base plate eigenmodes excited by acoustic noise. We discuss how to increase the natural frequencies of the base plate eigenmodes and determine the mode shape that is least likely to transmit vibrations to the specimen. We developed a new base plate with mode shapes that transmit the least amount of vibration. To confirm the improvement in performance, we installed our base plate on a SEM and compared the image noise amplitudes excited by acoustic noise with the results measured using the conventional base plate.

2. The SEM and Excitation of Image Noise

2.1 SEM

Figure 1 shows the general SEM principles. An electron beam is generated by an electron gun, concentrated through a condenser lens, and directed to a certain point on the specimen. The intensity of the secondary electron emission is measured by a detector. The intensity of the electrons is dependent on the type of material and its shape; these differences generate contrast. An image of the specimen is

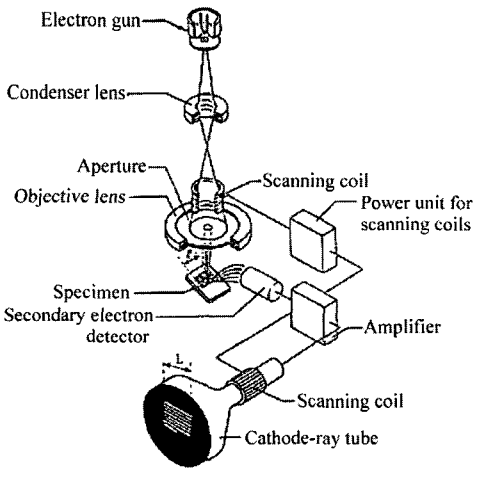

Fig. 1 SEM principles

formed from a two-axis scanning of the electron beam.

2.2 Influence of Vibrations on SEM Images

The relative displacement between the electron beam and the specimen cause fluctuations in the SEM images that we refer to as im age noise. The noise is caused by both the vibration transmitted from the floor and by structural vibration due to acoustic noise. The i mage noise disturbs the observed shape. A SEM that is less sensitive to these disturbances is highly desirable.

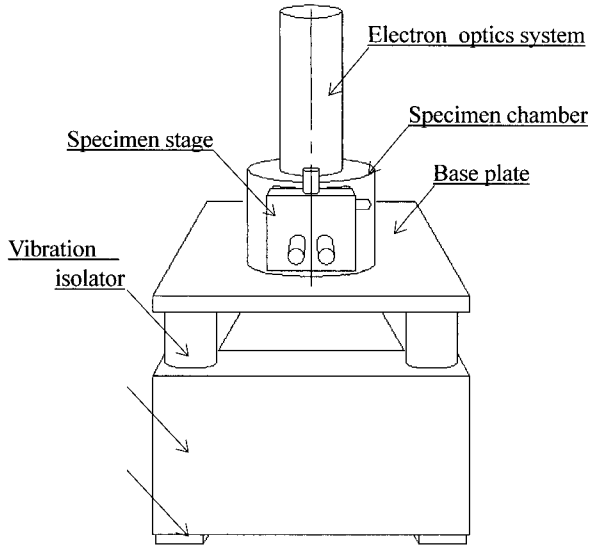

Fig. 2 Main structure of a SEM

We first describe the structural vibration that induces the image noise. Figure 2 shows the principal SEM components. The electron optics system that generates the electron beam and controls the position of the beam irradiation is located in the specimen chamber. The specimen stage that holds and moves the specimen is mounted in this chamber, which is fixed to the base plate. These structures ride on vibration isolators that reduce the transmission of floor vibrations. The isolators are placed on a frame that is set on the floor on rubber feet. The natural frequencies of these isolators are in the range of 1 to 3 Hz, so they decrease floor vibrations of higher frequencies. Although not shown in the figure, the specimen stage has three translation axes and two rotation axes. Since the specimen stage is connected by several mechanisms, there are many eigenmodes excited by disturbances around the equipment. These vibrations cause the image noise.

Next, we describe the mechanism by which the floor vibrations and vibrations excited by acoustic noise are transmitted to the SEM structures and cause image noise. Figure 3 shows the factors involved in the transmission of vibrations from the floor and from acoustic noise. The floor vibrations are transmitted mainly to the frame through the rubber feet, attenuated by the vibration isolators, and transmitted to the base plate, specimen chamber, and specimen stage. Other paths also exist. For example, electric signal lines, evacuation bellows, and water cooling tubes are directly connected to the base plate from the floor.

Acoustic noise impinges on all surfaces of the SEM and is transmitted to the specimen as vibrations. The frequency of the noise transmitted to the specimen is the result of multiplying the noise spectrum by the response functions of the components such as the base plate through which the vibrations pass.[1] The frequency profiles are different for the vibrations from the floor. While there are some elements shown in Fig. 3 that do not appear in Fig. 2, they are not discussed here because they are not relevant.

The aim of this paper is to reduce the image noise caused by the eigenmodes of the specimen stage. The natural frequencies of the stage that cause image noise are in the range of 100 to 200 Hz. Any floor vibration in this range is sufficiently attenuated by the vibration isolators. Acoustic noise, however, directly impinges on the structures above the isolators. Vibrations higher than 100 Hz are not attenuated, and they contribute to image noise more easily than floor vibrations do. In Section 3, we explain how the eigenmodes of the base plate, which has a relatively large area exposed to acoustic noise, are excited by acoustic noise. We also describe countermeasures that can be applied.

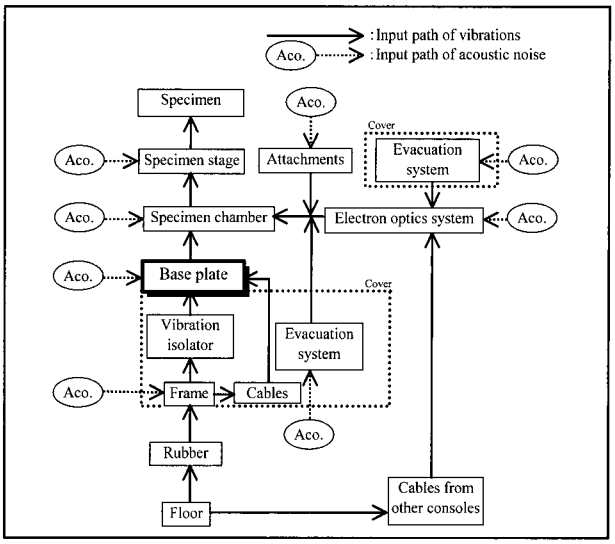

Fig. 3 Transmission model of SEM vibrations

3. Mode Shaping of the Structure

3.1 Force Input from Acoustic Noise

Figure 4 shows a model of how the acoustic noise causes SEM vibrations. The acoustic noise is a fluctuation of the atmosphere. When a sound source is placed above the center of the SEM, for example, the phase of the sound wave is different above and beneath the base plate, causing the plate to vibrate vertically. The maximum force exists when the phase difference is 180°. In the figure, the curves show the same phase of the sinusoidal sound, where the solid lines represent the maximum sound pressure, the dash-double-dotted lines are the minimum sound pressure, and the dash-dotted lines are the mean sound pressure. The velocity of sound is approximately 340 m/s at room temperature, and the base plate is 1 m long. Thus, the frequency of the sound whose phase is opposite above and below the plate is about 340 Hz. Sounds around this frequency can easily exert a force on the base plate. Sounds of lower frequencies that have wavelengths sufficiently longer than the length of the equipment exert the same phase on all the surfaces and thus do not affect the equipment.

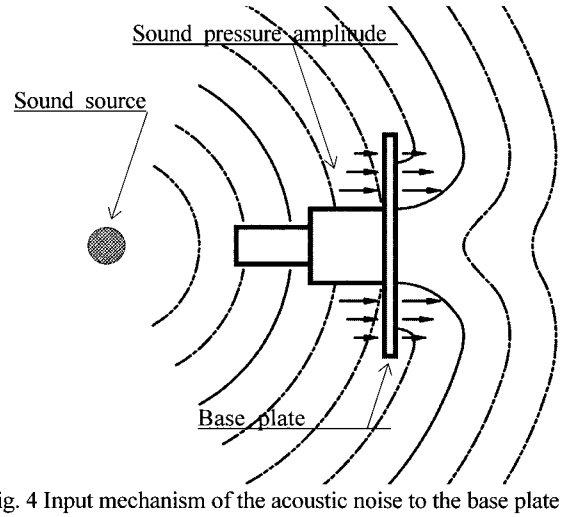

Fig. 4 Input mechanism of the acoustic noise to the base plate

3.2 Restriction of the Resonance

The eigenmodes of the specimen stage exist in the range of 100 to 200 Hz. When the eigenmodes of the base plate also exist below 200 Hz, the resonance of both the plate and the stage interfere with each other, resulting in a larger vibration to the stage. This is known as the octave law.[2] This resonance will be reduced if the natural frequency of the stage is twice that of the base plate, *i.e.*, if the frequencies of the eigenmodes are far from each other. However, it is difficult to increase the natural frequencies of the specimen stage because of its complexity. Therefore, we reversed the problem and attempted to reduce the vibration of the stage by making the natural frequencies of the plate higher than those of the stage. Thus, the target frequency of the first eigenmode of the plate was more than 200 Hz.

3.3 Structural Mode Shaping of the Base Plate

The natural frequencies of the plain rectangular base plate shown in Fig. 2 are proportional to the square root of the Young's modulus of the material and to the thickness of the plate. Therefore, to increase the natural frequencies of the plate, we must increase the thickness or change the material to one that has a higher Young's modulus. However, the plate mass increases in proportion to its thickness. A material that has a higher Young's modulus and lower density, such as a ceramic, will increase the cost. Therefore, a rib structure is often used instead of a more expensive material or an increased plate thickness.

It is possible to change the natural frequencies by adding ribs to increase the stiffness. However, it is impossible to change the mode shapes significantly. The lower frequency eigenmodes of a rectangular plain plate are the twisting mode, bending mode parallel to the major axis, and bending mode parallel to the minor axis. The formulas for calculating the natural frequencies of the rectangular plate were explained in detail by Leissa[3], and various boundary conditions apply.[4] However it is impossible to derive a formula for a complicated structure. Capitalizing on recent advances in computer simulation,[5,6] we used the finite element method (FEM), where it is quite easy to calculate and modify the natural frequencies and mode shapes of complicated structures,[7-11] and practically applied.[12-14] Thus, we could easily confirm the results for the rib added to the base plate at a variety of positions. We sought a structure that transmitted less vibration to the specimen, not only by from the perspective of the natural frequencies, but also in terms of the mode shapes. When the specimen chamber is placed on the vibration node of the base plate, less vibration will be transmitted to the chamber and the specimen. For example, the first mode is twisting, and two nodes are appeared on the centerlines parallel to the major and minor axes of the plate. When the specimen chamber is placed near the crossover point of the two nodes, the vibration at the first mode has low transmissibility to the chamber. However, the second mode is bending parallel to the major axis, and the center area of the plate is no longer the node in this mode. Thus, the vibration at the second mode is more easily transmitted to the chamber than that at the first mode.

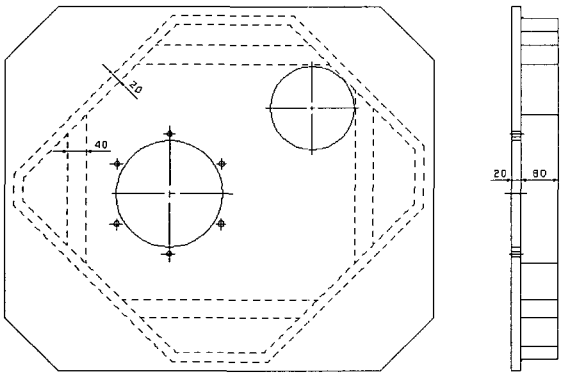

Fig. 5 Structure of the developed base plate

From this perspective, it is possible to reduce the transmissibility of the second mode by forming a node in the center area of the plate. In this case, the modes that have large transmissibility will be seen at the third mode, which has a higher natural frequency, and it is easier to make the third natural frequency higher than that of the specimen stage. Thus, we need to find where the rib should be placed to add the second twisting mode. From the infinite number of possibilities of forming other orthogonal twisting axes, we used those that lay on a 45° angle with the edges of the plate. We added an octagonal (almost rectangular) rib frame to the plate to produce these orthogonal nodes. The twisting mode of the rib frame had two orthogonal nodes parallel to the edges of this frame. The base plate was given a second twisting mode by adding this rib frame, which made a 45° angle with the edges of the plate. This frame also increased the stiffness of the first twisting mode and helped increase its natural frequency. Figure 5 shows the base plate incorporating this concept. The top plate was 20 mm thick and the four corners were cut. Doubled octagonal rib frames 80 mm high were fixed below the plate. The width of the outer rib was 20 mm, and that of the inner rib was 40 mm. This rib shape was simple so it could be easily welded to the plate.

The large hole shown in the center of the plate was used to attach the specimen chamber. A second smaller hole was used to route the electric cables. The reason for cutting the four corners was to increase the natural frequency of the twisting mode of whole base plate. The vibration isolators were placed below these areas; the areas outside of the isolators were useless. With the corners removed, the inertia around the twisting nodes decreased, and the natural frequency of the twisting mode increased by 10%. The role of the inner rib was to increase the natural frequency of the twisting mode of the outer rib frame. The structure shown in Fig. 5 has two twisting modes due to the octagonal rib: the twisting of the whole base plate, and the twisting of the rib frame. Each node of these modes crossed the others near the center of the plate. Since the specimen chamber was placed at the center of the plate, the transmissibility of the vibration from the base plate to the chamber was reduced.

3.4 Evaluation of the Base Plate

3.4.1 Comparison of Eigenmodes

Figure 6 shows the natural frequencies of the plain plate calculated up to the 4th mode using a FEM analysis. The solid lines show the structural shape while the dashed lines show the mode shape. The 1st mode was twisting, and 2nd and 3rd modes were bending along the major and minor axis respectively. The 4th mode was also twisting with one node (shown as line *c* in the bottom right of Fig. 6) parallel to the major axis, and two nodes (shown as lines *a*

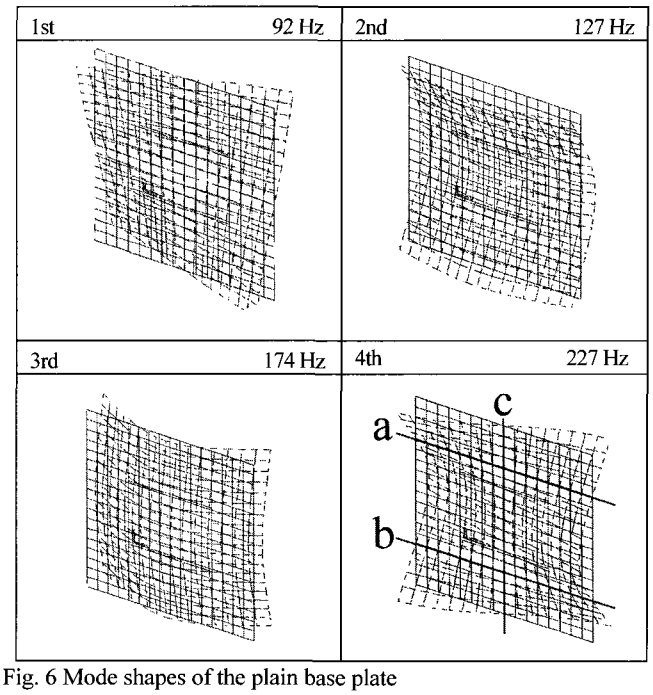

Fig. 6 Mode shapes of the plain base plate

and *b*) parallel to the minor axis. Figure 7 shows the mode shapes of the base plate we developed with the improved rib. For clarity, this figure also shows the vibration models of each mode on the right-hand side.

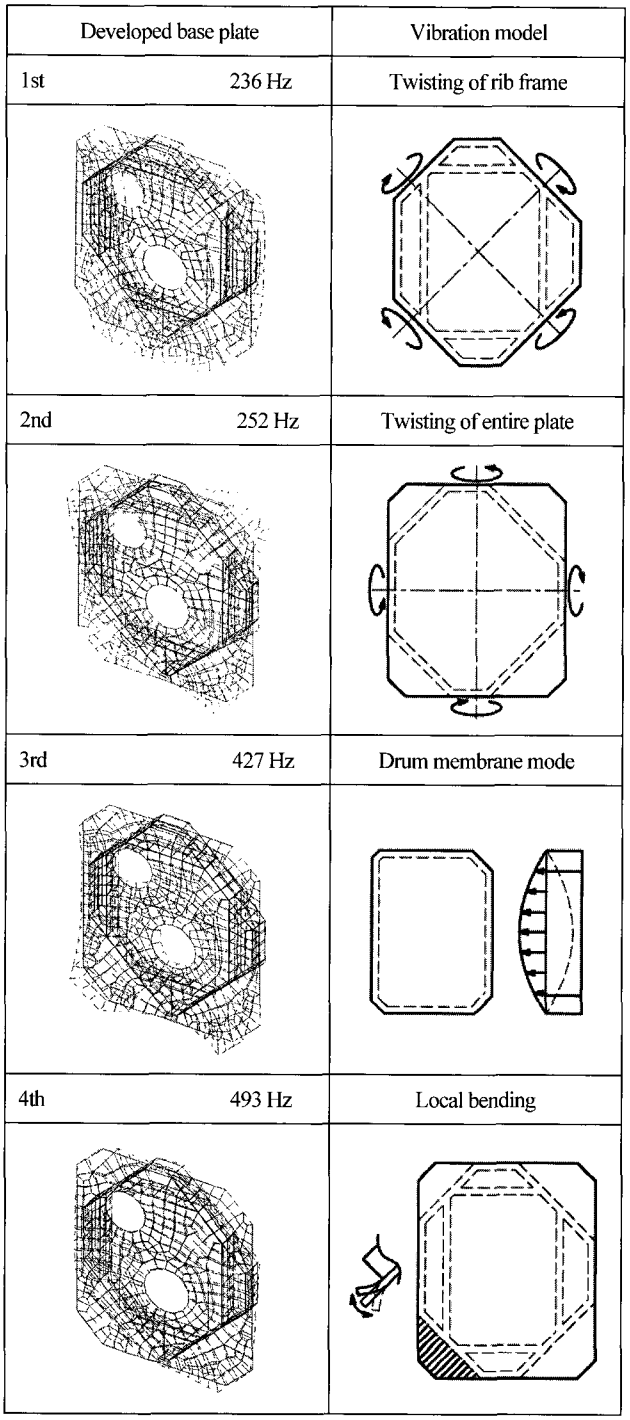

Fig. 7 Mode shapes of the developed base plate and vibration models

Our objective was to increase the frequency of the 1st mode to a value greater than 200 Hz, but we actually achieved 236 Hz. This mode corresponded to twisting of the rib frame. The amplitude around the center hole where the chamber is mounted was smaller than outside. The 2nd mode (252 Hz) corresponded to twisting of the whole base plate. Thus we succeeded in reducing the transmission of vibrations excited in the two modes. In the 3rd mode (427 Hz), the area inside the rib frame vibrated like the membrane of a drum, and the amplitude at the center was large. However, compared to the bending mode (127 Hz) with the plain base plate, which had a relatively large amplitude in the center area (see Fig. 6), the natural frequency of the developed base plate was three times higher than that of the plain base plate. The 4th mode (493 Hz) was a local bending mode of the area outside the rib frame, shown at the right side of the fourth row in Fig. 7. There were also similar local modes in the other three areas outside the rib frame. The shapes of these four areas were different from each other so that they had different natural frequencies. If they were equal to each other, the vibrations would be excited simultaneously at that frequency, producing a much larger amplitude at the center of the plate. Thus, having different shapes for these areas avoided large vibrations in the presence of sinusoidal acoustic noise at the frequency of the local modes.

These results were obtained from our simulations. To confirm the eigenmodes, we produced a physical specimen of the developed base plate and conducted a modal analysis of it using the impulse method. Analyses of the base plate were conducted as components and then assembled. The results are shown in Table 1. In the table, the first row shows the simulated values for the developed base plate while the second shows the measured value for the developed base plate before assembly. The third row shows the measured value for the developed base plate once all the components had been assembled on it, and the fourth row shows the measured value of the plain base plate with the components assembled on it. The natural frequencies for the 1st, 2nd, and 3rd modes are shown for each. Here, the 1st mode is the twisting of the whole base plate and 2nd mode is the twisting of the rib frame, which is the reverse of the simulation. To compare the frequencies, the order of the modes was inverted. The reasons for the difference between the simulated values shown in the first row in Table 1 and the measured unassembled values shown in the second row are the accuracy of the calculations and the effect of welding the rib. However, the differences were not more than 10%. The differences between the measured frequencies for the unassembled and assembled components shown in the second and third rows were caused by the chamber and other structures. The first natural frequency of the assembly was greater than 250 Hz, about three times higher than that of the plain base plate, achieving the aim of increasing it over 200 Hz. The weight of the plain base plate was 100 kg, while that of the developed one was 165 kg. To increase the natural frequency by three times without using a rib would have required a plate three times as thick and three times heavier. From that perspective, the mass increase of the developed base plate was three times smaller than it would have been with a plain plate. In summary, a new base plate was developed with two twisting modes as the first two modes. In those modes, the vibration transmission to the specimen chamber was small because they were located on each node of the eigenmodes.

3.4.2 Image Noise Amplitude Due to Acoustic Noise Exposure

The amplitude of the image noise when exposed to acoustic noise was compared for the original and the developed base plates. The acoustic exposure was provided by a speaker system 1 m from the SEM and 1 m off the floor. SEM images were captured under acoustic exposure. The sound sources were sinusoidal waves and a 1/3 octave band filtered pink noise. The frequencies of the sinusoidal wave were varied from 100 to 200 Hz in 2 Hz steps. The center frequency of the 1/3 octave band noise was in the range of 50 to 1000 Hz. The sound pressure level was 75 dB (flat scale in equivalent sound pressure level) in all experiments, and the level of the background noise was about 60 dB. Figure 8 shows examples of images exposed to sinusoidal waves at 160, 162, and 164 Hz. The images were captured scanning from the left to right, line by line, top to bottom. Each image required 80 s to capture. During the image capture, the frequency was changed twice, from 160 to 162 Hz and from 162 to 164 Hz at the points shown by the horizontal white lines. Since the sizes of the specimen particles were different, the sections appear different although they were captured at the same magnification, as shown in the white bar scale for 100 nm in each part of Fig. 8. The image noise amplitudes were measured at the edges of the particles where there was sufficient contrast. However, it was difficult to measure the vibration component that crossed perpendicular to the scanning beam. Therefore, the amplitude of the

image noise was measured as follows. Figure 9 shows images captured with the bean scanning rotated by 90°. In the two images, the amplitude of the image noise was measured where the edges were perpendicular to the beam scanning direction at five points, and the values were averaged. The amplitude of the image noise was defined as the root mean square value of the two averages. Figures 8 and 9 show that the images obtained using the plain base plate were clearly affected by the noise, while there were almost no noise effects on the developed base plate.

Table 1 Natural frequencies of the base plates

Type	1st mode	2nd mode	3rd mode
Developed (calculated)	252 Hz	236 Hz	427 Hz
Developed (unassembled)	240 Hz	263 Hz	408 Hz
Developed (assembled)	253 Hz	293 Hz	333 Hz
Plain (assembled)	84 Hz	125 Hz	153 Hz

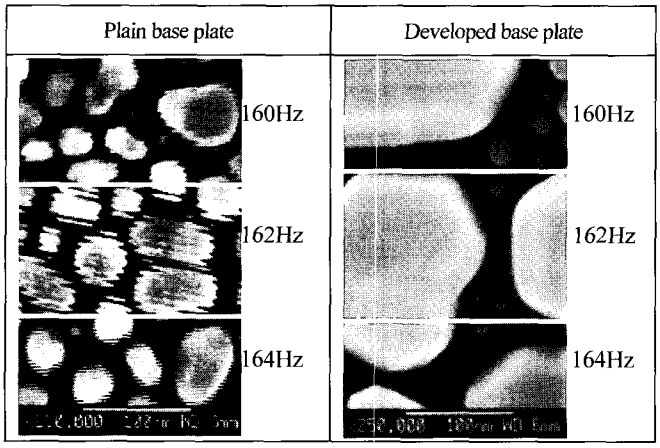

Fig. 8 SEM images exposed to sinusoidal acoustic noise from 160 to 164 Hz

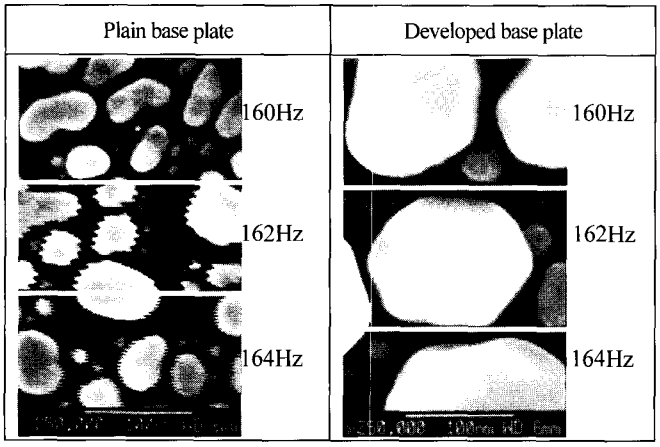

Fig. 9 SEM images exposed to sinusoidal acoustic noise from 160 to 164 Hz (90° scan rotated)

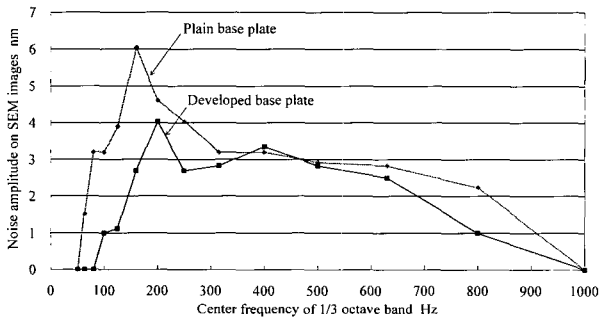

Fig. 10 Noise amplitude on SEM images exposed to a 1/3 octave band acoustic noise

The differences in the image noise were compared when the plates were exposed to the effects of 1/3 octave band noise. As with the sinusoidal wave tests, two images rotated at 90° were captured and the amplitude of the image noise was measured. There was a significant decrease in the noise with the developed base plate for frequencies below 250 Hz. This means that the transmission of vibrations to the specimen stage was restricted because there was no eigenmode below 250 Hz. Although the developed base plate had an eigenmode at 253 Hz when assembled, as shown in the third row of Table 1, Fig. 10 indicates that the image noise at 250 Hz had decreased. This is because the area on which the specimen chamber was placed corresponded to the node of this twisting mode so that less vibration was transmitted to the chamber. There were no remarkable differences above 250 Hz. In many cases, the frequency profiles of the sound pressure level had smaller values at higher frequencies. Thus, having less image noise at lower frequencies is beneficial for a SEM. The developed base plate has already been applied to products on the market. Previously, when observations at high magnification were required under higher sound pressure level conditions, an acoustic shield box was often used, but this was heavy and cumbersome. The new base plate has reduced the number of times when the box has been required, and hence contributed to better performance at lower cost.

4. Conclusions

We studied the transmission path of vibrations that cause image noise in a SEM. We examined the mode shapes that reduce the transmission of acoustic noise vibration through the base plate. To avoid the natural frequencies of the plate that were too close to the specimen stage, the target frequency of the first eigenmode was greater than 200 Hz.

We developed a new base plate and measured the natural frequencies and mode shapes. As a result, the frequency of the 1st mode increased to over 250 Hz. As intended, the 1st and 2nd modes were both twisting. We confirmed that the base plate transmitted less vibration to the specimen.

We compared the image noise captured using the plain base plate and the developed base plate under acoustic noise excitation. We observed a significant reduction of image noise for frequencies below 250 Hz.

The developed base plate[15] has already been applied to products on the market.

REFERENCES

1. Tokita, Y. and Morimura, M., "Handbook for Precise Isolation of Vibration," FUJI Techno System, p. 98, 1987.
2. Steinberg, D. S., "Practical Manual for Countermeasure of Vibration for Electrical Equipments," Japan Technical Economy Center, p. 286, 1983.
3. Leissa, A. W., "The Free Vibration of Rectangular Plates," J. Sound Vibration, Vol. 31, No. 3, pp. 257-293, 1973.
4. Sekiya, S., Hamada, M. and Kaku, S. "Handbook for Design of Plates' Stiffness," Asakura Publishing, p. 141, 1982.
5. Chen, T. Y., "Structural Modification with Frequency Response Constraints for Undamped MDOF Systems," Computers and Structures, Vol. 36, Issue 6, pp. 1013-1018, 1990.
6. Wang, X., Zhou, J. and Hu, Y., "A Physics-Based Parameterization Method for Shape Optimization," Computer Methods in Applied Mechanics and Engineering, Vol. 175, Issue 1-2, pp. 41-51, 1999.
7. Sestieri, A. and D'Ambrogio, W., "A Modification Method for

Vibration Control of Structures," Mechanical Systems and Signal Processing, Vol. 3, Issue 3, pp. 229-253, 1989.

8. Park, Y. H. and Park, Y. S., "Structure Optimization to Enhance its Natural Frequencies Based on Measured Frequency Response Functions," J. Sound Vibration, Vol. 229, Issue 5, pp.1235-1255, 2000.
9. Lee, J. S., "Automated Structural Design System Using Fuzzy Theory and Neural Network," International Journal of Precision Engineering and Manufacturing, Vol. 3, No. 1, pp. 43-48, 2002.
10. Chae, J. S., Park, T. W. and Kim, J., "Dynamic Analysis of a Flexible Multibody System," International Journal of Precision Engineering and Manufacturing, Vol. 6, No. 4, pp. 21-25, 2005.
11. Chung, I., "Evaluation of Effective Stiffness for 3D Beam with Repeated Structure," International Journal of Precision Engineering and Manufacturing, Vol. 7, No. 2, pp. 25-29, 2006.
12. Done, G. T. S. and Rangacharyulu, M. A. V., "Use of Optimization in Helicopter Vibration Control by Structural Modification," Journal of Sound and Vibration, Vol. 74, Issue 4, pp. 507-518, 1981.
13. Holmes, J., "Mode Shape Corrections for Dynamic Response to Wind," Engineering Structures, Vol. 9, No. 3, pp. 210-212. 1987.
14. Alejandro, J. R. and Marc, P. M., "Maximum Amplification of Blade Response due to Mistuning: Localization and Mode Shape Aspects of the Worst Disks," Journal of Turbomachinery, Vol. 125, Issue 3, pp. 442-454, 2003.
15. Hamochi, M., "Base Plate for Isolation of Vibration," JEOL Ltd., JP 3581257, 2004.